Influence of poly(butylene terephthalate) and wollastonite on properties of recycled poly(ethylene terephthalate) preforms

Phasawat CHAIWUTTHINAN[1], Thaksaporn RIYAPHAN[2], Athapon SIMPRADITPAN[2], and Amnouy LARPKASEMSUK[2,*]

[1] MTEC, National Science and Technology Development Agency (NSTDA), Thailand Science Park, Khlong Luang, Pathum Thani, 12120, Thailand
[2] Department of Materials and Metallurgical Engineering, Faculty of Engineering, Rajamangala University of Technology Thanyaburi, Pathum Thani 12110, Thailand

*Corresponding author e-mail: amnouy.l@en.rmutt.ac.th

Abstract

Influence of poly(butylene terephthalate) (PBT) and wollastonite (WLN) on properties of recycled poly(ethylene terephthalate) (RPET) was investigated. RPET was first melt-mixed with PBT at five loadings (10-50 wt%) on a twin screw extruder, and then injection molded. Scanning electron micrographs showed the immiscible blends. The blends at 10-40 wt% PBT displayed droplet-matrix morphology, while the blend at 50 wt% PBT showed a matrix inversion. All blends showed a PBT-dose-dependent increase in impact strength and Young's modulus with an expense of tensile strength and elongation at break. Among five RPET/PBT blends, the one at 40 wt% PBT exhibited the good balanced mechanical properties in terms of toughness and stiffness, which was subsequently filled with four loadings of WLN (10-40 wt%). The addition of WLN showed a noticeable increase in the impact strength and Young's modulus, especially at 30 wt% WLN, and a slight reduction in the tensile strength and elongation at break. The composite at 30 wt% WLN exhibited a better dispersion of WLN in polymer matrix and wettability between polymers and WLN, leading to the higher mechanical properties. Differential scanning calorimetry revealed the miscibility of RPET and PBT in amorphous region and the immiscibility in crystalline phase.

1. Introduction

Poly (ethylene terephthalate) (PET) and poly(butylene terephthalate) (PBT) are among the aliphatic-aromatic polyesters of prime commercial and industrial importance that are extensively used in packaging, textile, electrical part and automotive component part industries due to their excellent mechanical, thermal and chemical properties [1-11]. Recently, PET becomes the preferred material over glass and metal in packagings, in particular for short-term applications because of its lightweight, high clarity, high strength, high dimensional stability and good barrier properties, excellent chemical resistance, and easy recyclability [1,3-7]. It occupies an important market in the manufacturing of bottles for drinking water and carbonated beverage. The ever-increasing production and utilization of PET lead to the depletion of petroleum resources and the intensive accumulation of the used products in the waste stream due to its non-biodegradability and high atmospheric resistance [1,2,4,8]. However, PET is known as one of the most recyclable thermoplastics, and the mechanical recycling is an important technique that not only reduces the amount of PET waste in landfills but also conserves the raw petrochemical products and energy [4]. It is to reintegrate PET waste into the production cycle as a raw material for manufacturing various products using conventional processing techniques. This concern has attracted a number of research interests in both academic and industrial sectors to explore various recycling techniques to handle waste PET. The recycled PET (RPET) used in this study is the discarded preform scrap obtained from the plastic bottle manufacturing process, which is an industrial waste. Therefore, it is more convenient to recycle and also yields better performance properties than the post-consumer packaging wastes because of its easy collection and segregation and less contamination. However, the application of the RPET products may have some limitations depending on the properties of resin and the extent of thermal and hydrolytic degradations during processing [1]. To diversify and upgrade the recycled products, blending RPET with other polymers and/or fillers, such as poly(lactic acid) [8], polypropylene (PP) [5,11], poly(butylene adipate-co-terephthalate) [1,4,12], PBT [3], poly(butylene succinate) [9], polycarbonate [13,14], high density polyethylene [15], nitrile rubber [16], nanoclay [6,8], wood flour [12], short glass fiber [17], wollastonite (WLN) [4,5,9], and talc [10] has been proposed in literatures.

Influence of poly(butylene terephthalate) and wollastonite on properties of recycled poly(ethylene terephthalate) preforms

125

Nofar and Oğuz [3] reported the preparation and properties of RPET/PBT blends at three different weight ratios (75/25, 50/50 and 25/50). The results showed that the blends were fully miscible in the amorphous region and their molecules could co-crystallize and be fully miscible in crystalline phases only upon slow cooling of the melt. The melt strength loss of the RPET after processing could be regained by the addition of PBT. It was further observed that the impact strength of the blends was slightly increased with increasing PBT content, while the elongation at break was remarkably decreased and the Young's modulus did not differ with that of the PBT. Chaiwutthinan et al. [5] investigated the influence of WLN on mechanical, thermal and morphological properties of the RPET/PP blends. The results showed that the tensile strength, Young's modulus, and heat distortion temperature of the blend composites were all improved in a WLN-dosed dependent manner, while the impact strength and elongation at break slightly decreased.

In this study, RPET was melt blended with a commercial PBT. The interest in using PBT arises from its unique properties as engineering thermoplastic polyester, having interesting balance of desired properties, such as high toughness, flexibility, resistance to fats and all organic solvents, and easy processability [2,3,18-20]. Their blends are expected to be highly miscible (in amorphous phase) without requiring any compatibilizer because of their quite similar chemical structures [2,3,21,22]. Both of them belong to a series of homologous aromatic-polyesters, which differ in the backbone units only by two or four methylene groups of PET and PBT, respectively [21]. Generally, thermal and chemical resistance and mechanical properties of PBT are comparable to those of virgin PET, but impact strength and rate of crystallization are higher [22]. The difference in crystallization rates may reduce the miscibility between RPET and PBT after being quenched in the injection molding process [3], which consequently lowers the mechanical and thermal properties of the resulting blends. Meanwhile, the application of RPET is often limited due to the deterioration of its properties caused by thermomechanical degradation during reprocessing. To overcome these deficiencies, the blend with optimum combination of mechanical properties was further reinforced with different loading levels of WLN, which is a calcium metasilicate ($CaSiO_3$) mineral occurred naturally in an acicular (needle-shaped) crystal structure with a high aspect ratio (L/D of 10-20), as shown in Figure 1 [4,5,20]. It is mainly comprised of CaO (~48.25 wt%) and SiO_2 (~51.75 wt%) [4,5] with many desirable properties, such as high chemical and thermal stability, high level of whiteness and hardness (Moh's hardness 4.8), small health hazard compared to asbestos, and very low cost [4,5,20]. With this respect, the mechanical, thermal, and morphological properties of the resulting products were comparatively investigated.
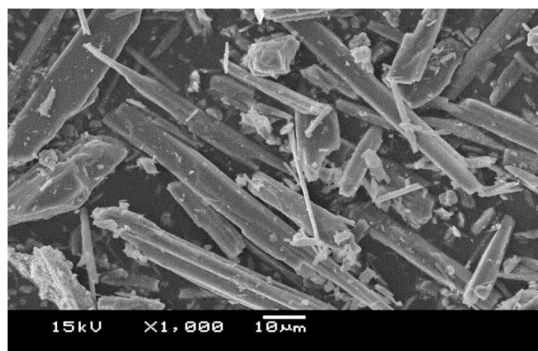
Figure 1. Representative SEM image of the WLN particles (×1,000).

2. Experimental

2.1 Materials

The RPET flakes were obtained from waste preform in plastic bottle manufacturing process. Commercial PBT (Duranex® 2092 FF2001) pellets with a density of 1.46 g·cm^{-3} and a heat distortion temperature of 110°C were purchased from the Polyplastic Co., Ltd. (Japan). Ultrafine WLN (XYNFW-XA) with an average particle size of 5 μm and a density of 2.85 g·cm^{-3} from China was supplied by the Pacific Comma Trading Company (Thailand).

2.2 Sample preparation

RPET flakes, PBT pellets and WLN powder were oven-dried separately at 120°C for 4 h to remove any trace of moisture prior to compounding. The RPET/PBT blends (90/10, 80/20, 70/30, 60/40 and 50/50 (wt%/wt%)) were first prepared by melt blending on a Barbender CTE-D02L800 co-rotating twin-screw extruder (UK), having a screw diameter of 15.75 mm, L/D ratio of 32 under a temperature profile of 200, 260, 265 and 245°C from the feed zone to the die head at a fixed screw rotational speed of 75 rpm. The obtained extrudates were subsequently pelletized, dried at 140°C for 4 h, and then fabricated into the standard impact and tensile test specimens using an Arburg Allrounder 470C Golden injection molding machine (Germany) under a temperature profile of 255, 275, 280, 285 and 300°C from the feed zone to the die head at an injection speed of 10 cm^3·sec^{-1} and injection pressure of 1050 bar.

The RPET/PBT/WLN composites were also prepared by the melt blending and injection-molding process as described above but with the incorporation of one of four loadings of WLN (10, 20, 30 and 40 wt%).

2.3 Characterization

The notched Izod impact test was conducted on a standard test sample (12.7×63.5×3 mm^3) using a Ceast

9709 impact tester (Italy) according to ASTM D256. The tensile test was performed on a standard dumbbell-shaped specimen according to ASTM D638 (Type I) using a Hounsfield H 50 KS universal testing machine (UK) with a 10 kN load cell and a crosshead speed of 50 mm·sec^{-1}. The value of each property was obtained from the average of at least five specimens for each composition.

The morphology of the impact fractured surface was observed on a Jeol JSM 6510 SEM (Japan) at an accelerated voltage of 15 kV and a magnification of 3,000x. Prior to observation, the fractured surface was sputter-coated with a thin layer of gold (~20 nm) to avoid electrostatic charges occurred during examination.

The thermal and crystallization behaviors of the samples were determined by a Netzsch DSC 200 F3 analyzer (Germany) under a nitrogen atmosphere mL·min^{-1}. The sample (about 10 mg) was placed in aluminium sample pan and heated from 0 to 350°C (first heating run) and held isothermally for 2 min to erase any previous thermal history of the material and then cooled down to 0°C (cooling run). The sample was reheated to 350°C (second heating run) and then cooled down to room temperature. All measurements were conducted at the same heating/cooling rate of 10°C·min. The glass transition temperature (T_g), crystallization temperature (T_c), cold crystallization temperature (T_{cc}), and melting temperature (T_m) were reported.

3. Results and discussion

3.1 Mechanical properties

The experimental data related to the mechanical properties (impact strength, tensile strength, elongation at break, and Young's modulus) of all the investigated samples are listed in Table 1. The impact strength values of the neat RPET and PBT were 20.5 and 49.5 J·m^{-1}, respectively. The direct addition of PBT at 10 and 20 wt% to the RPET exhibited a small decline in the impact strength of the blends (10.7 and 7.3%, respectively) compared to that of the neat RPET. This may be due to a deficient dispersion of PBT in the RPET matrix, leading to a poor stress transfer across each phase. However, the impact strength of the blend at 30 wt% PBT was slightly increased by 8.3% over that of the neat RPET, and noticeably increased by 22 and 29.3% at 40 and 50 wt% PBT, respectively. This suggested that the PBT offered its high impact strength to the RPET only at high loading levels, attributing to a better PBT dispersion within the RPET matrix at these concentrations, which in turn increased the better stress transfer at the interface of the RPET and PBT. However, the optimal impact strength at 50 wt% PBT may be the result of matrix inversion, which could be confirmed later by the SEM analysis. Meanwhile, the elongation at break values of both RPET and PBT were rather low and were in the same level (4.8 and 4.4%, respectively) due to the hard polyester segments induced by the aryl groups in their structures, which

limited the polymer chain mobility. The elongation at break of the blends (2.2-3.5%) was not improved compared to that of the neat RPET and PBT, but rather was lower. As expected, the tensile strength values of all the blends were found to be lower than that of the neat RPET (0.5-38.6%) because of the lower tensile strength of PBT. However, the tensile strength of the blends showed an increasing trend with increasing PBT content, but at the highest PBT loading of 50 wt%, a decreasing tensile strength was evidenced, which may be due to the phase reversion as mentioned above. Moreover, all the blends exhibited a dose-dependent increased Young's modulus (12.3-39.4%) compared to the neat RPET (1757.7 MPa) due to the higher Young's modulus of PBT (2302.3 MPa). It is also seen that the Young's modulus increased up to the maximum value at 40 wt% PBT, attributing to a higher chain entanglement or physical crosslink between RPET and PBT that strongly obstructed the mobility of the polymer chains during deformation. These findings suggested that the PBT improved not only the toughness but also the stiffness of the blends, particularly at the PBT loading of 40 wt%. Hence, the 60/40 (wt%/wt%) RPET/PBT blend with good combination of the mechanical properties in terms of stiffness and toughness was then selected for preparing composites with four loading levels of the ultrafine WLN (10-40 wt%).

The mechanical properties of the resulting RPET/PBT/WLN composites are presented in Table 1 and Figure 2. Interestingly, the impact strength values of all the composites (36.3−77.7 J·m^{-1}) were much higher than that of the neat blend (25 J·m^{-1}), indicating that the composites were much tougher than the neat blend. This may be due to the high aspect ratio (10-15) and specific surface area of the WLN particles that gave rise to a high stress transfer between the WLN and polymer matrix [20]. Moreover, there existed a synergistic effect of PBT and WLN on absorbing the impact deformation energy under impact loading. However, the impact strength of the composites was found to increase up to the optimal value at 30 wt% WLN (Figure 2(a)), implying a better WLN dispersion in the polymer matrix at this loading level. A decrease in the impact strength of the composite at 40 wt% WLN may be due to the agglomeration of an excess WLN, leading to a decreased contact area between the filler and polymers that allowed less stress transfer across the phases. Meanwhile, the elongation at break values of the composites at 10-30 wt% WLN were higher than that of the neat blend and the composite at 40 wt% WLN.

However, the elongation at break of the composites decreased continuously with increasing WLN loadings (Figure 2(b)) due to the stiffness of WLN particles that restricted the mobility of the polymer chains and also the lower amount of polymer matrix that held the WLN particles together in the composites, which were in turn lower their elongation at break. In addition, the tensile strength of all the composites was slightly

lower than that of the neat blend due to the weak interfacial interaction between either the RPET or the PBT and the WLN particles. However, among these composites, the one at 30 wt% WLN exhibited the highest tensile strength (Figure 2(c)), indicating the better WLN dispersion in the polymer matrix at this concentration.

Meanwhile, the Young's modulus of the composite at 10 wt% WLN was slightly lower than that of the neat 60/40 (wt%/wt%) RPET/PBT blend due to an insufficient dispersion of WLN in the polymer matrix, but at the higher WLN loadings (20-40 wt%), the Young's modulus of the composites was found to be higher than that of the neat blend due to the good distribution of the stiff WLN particles in the polymer matrix that effectively restricted the mobility of the polymer chains during the tensile deformation, and again the composite at 30 wt% WLN exhibited the highest Young's modulus (Figure 2(d)).

Table 1. Mechanical properties of the samples.

Sample	Impact strength (J·m⁻¹)	Elongation at break (%)	Tensile strength (MPa)	Young's modulus (MPa)
RPET	20.5 ± 3.0	4.8 ± 0.5	61.6 ± 2.0	1757.7 ± 109.0
PBT	49.5 ± 1.0	4.4 ± 0.4	50.4 ± 1.0	2302.3 ± 203.5
RPET/PBT (wt%/wt%)				
90/10	18.3 ± 4.2	2.2 ± 0.5	37.8 ± 7.0	2312.5 ± 244.5
80/20	19.0 ± 2.0	3.0 ± 0.5	46.0 ± 5.7	1998.8 ± 155.5
70/30	22.2 ± 0.6	3.2 ± 0.5	53.2 ± 5.0	2284.7 ± 187.5
60/40	25.0 ± 0.5	3.2 ± 0.5	56.0 ± 6.6	2451.0 ± 218.5
50/50	26.5 ± 1.4	3.5 ± 0.3	49.3 ± 2.6	1974.0 ± 201.5
RPET/PBT/WLN (wt%/wt%/wt%)				
54/36/10	36.3 ± 3.9	5.5 ± 0.8	50.8 ± 0.6	2309.7 ± 59.8
48/32/20	45.0 ± 6.0	4.0 ± 0.7	52.3 ± 0.4	2613.5 ± 105.7
42/28/30	77.7 ± 5.4	3.6 ± 0.2	53.7 ± 0.3	2974.5 ± 136.3
36/24/40	39.5 ± 5.4	3.0 ± 0.3	53.0 ± 0.2	2901.3 ± 232.7
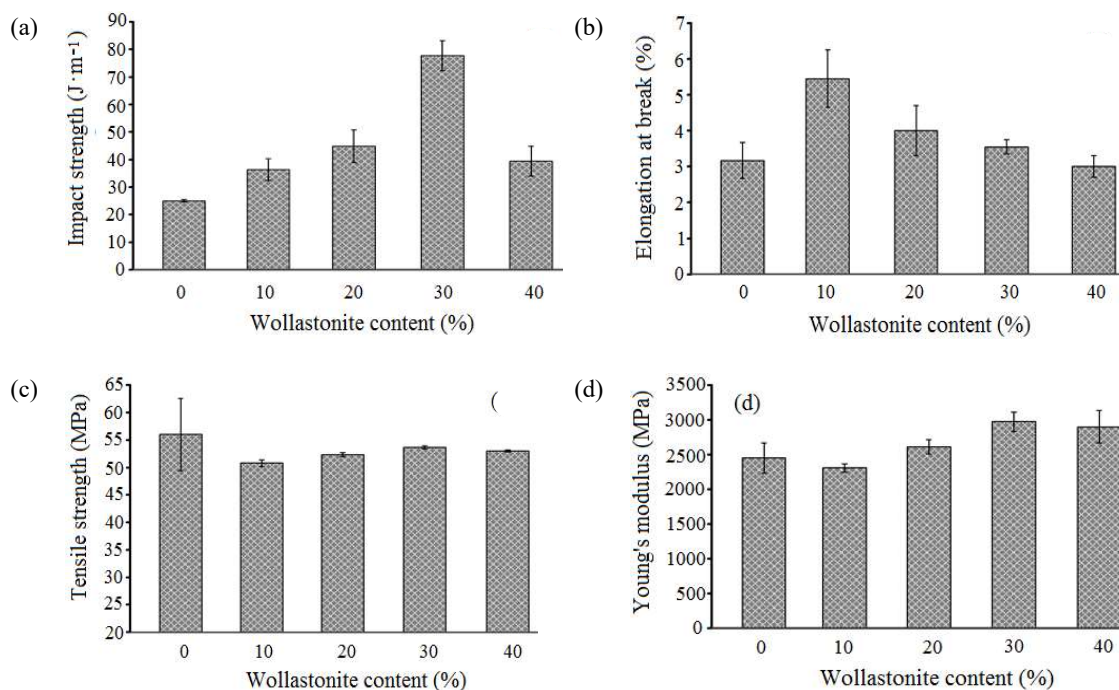
Figure 2. Mechanical properties of the composites as a function of the WLN content in terms of (a) impact strength, (b) elongation at break, (c) tensile strength and (d) Young's modulus.

3.2 Morphology

Representative SEM images at 3,000x magnification of the tensile fractured surface of the neat RPET and PBT and their five blends are shown in Figure 3. The neat RPET exhibited a relatively flat and smooth surface with some low ridges across the surface and without visible plastic deformation (Figure 3(a)), indicating that the sample fractured under a brittle mode, while the neat PBT showed a fine-grain morphology (Figure 3b) due to its high toughness, which was in agreement with a previous report [21]. However, the fractured surfaces of the RPET/PBT blends at 10-30 wt% PBT were relatively smooth as well (Figures 3(c-e)), indicating that these blends were still rather brittle. Meanwhile, the blend at 40 wt% PBT showed a relatively irregular fractured surface due to its more ductile fractured behavior (Figure 3(f)). Moreover, the blends at these concentrations (10-40 wt% PBT) showed two phases, droplet-matrix type morphology, where small droplets of PBT dispersed in the RPET matrix.

However, matrix inversion in immiscible RPET/PBT blend occurred at high PBT content (50 wt%) (Figure 3(g)), where the RPET dispersed phase was found to be entrapped in the PBT matrix. These findings were in good agreement with the previous results of the mechanical properties.

Representative SEM images of the investigated 60/40 (wt%/wt%) RPET/PBT blend composites with four different loading levels of WLN (1040 wt%) are all presented in Figure 4. Among them, the one at 30 wt% WLN revealed a better dispersion of WLN particles in the polymer matrix and also a better wettability between either RPET or PBT and WLN (Figure 4(c)), while the other composites showed clear boundaries and interstices between the WLN and the polymer blend matrix (Figures 4(a, b and d)). Thus, the WLN particles could serve as local stress concentrators under stress, leading to a decrease in their strength.
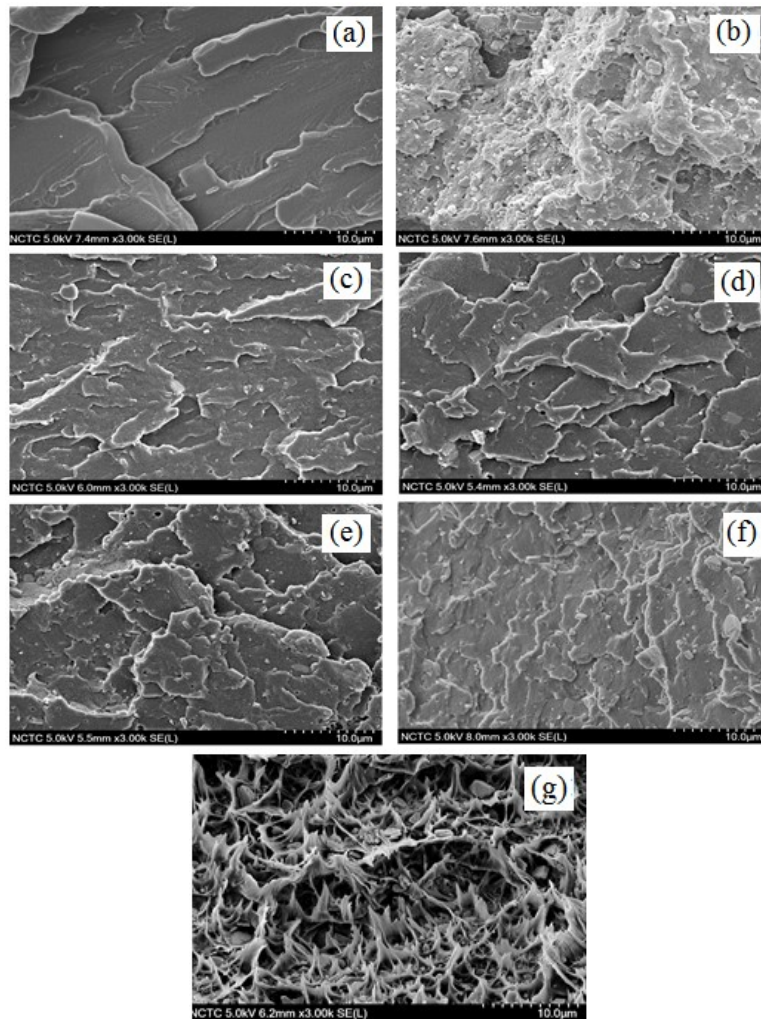
Figure 3. Representative SEM images (×3,000 magnification) of (a) RPET, (b) PBT and (c-g) RPET/PBT blends with PBT content at 10, 20, 30, 40 and 50 wt%, respectively.
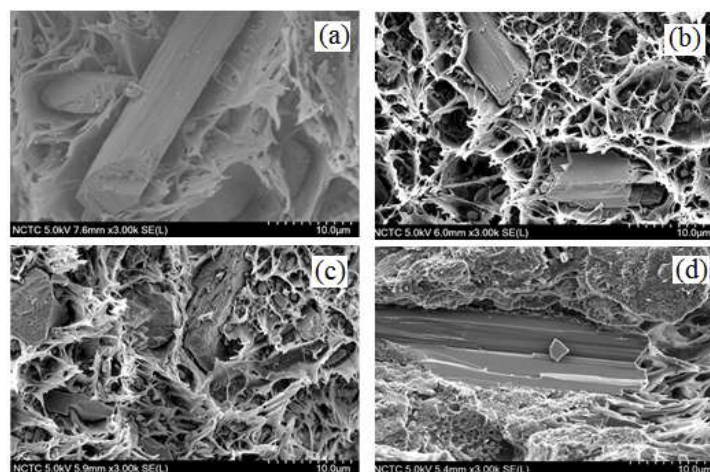
Figure 4. Representative SEM images (×3,000 magnification) of the composites with WLN content of (a) 10 wt%, (b) 20 wt%, (c) 30 wt% and (d) 40 wt%.

3.3 Thermal properties

Figures 5 and 6 show the representative DSC thermograms of the investigated samples derived from the first heating, cooling and second heating scans at a heating/cooling rate of 10°C·min^{-1}. Table 2 summarized the numerical values of their T_g, T_{cc}, T_m, and T_c.

From the first heating curves (Figure 5(a)), the neat RPET and PBT exhibited a T_g at 74.5°C and 60°C, respectively, indicating that RPET had higher T_g than PBT due to the short methylene groups in RPET that made it more polar than PBT, and thus required more energy for chain mobility [19]. However, a single T_g was observed for each RPET/PBT blend, which indicated their miscibility in the amorphous region [3,19]. Moreover, the T_g of all the blends (67-69.8°C) showed no significant difference and was lower than that of the neat RPET due to the lower T_g of PBT. The first heating curves in Figure 6(a) also revealed a single T_g for all the 60/40 (wt%/wt%) RPET/PBT blend composites with WLN, which was probably due to the miscibility between RPET and PBT in the amorphous region as well [11]. The T_g of all the composites was in the range of 60-63.7°C, which was lower than that of the neat blend (68°C). This is due to the weak interfacial adhesion and wettability between either RPET or PBT and WLN that facilitated the mobility of the polymer chains, as mention earlier in the SEM analysis. Meanwhile, the neat RPET exhibited a T_{cc} at 120°C (Figure 5(a)). The cold crystallization could be observed after the RPET molecules gained sufficient thermal energy and mobility to arrange themselves in a well-organized structure upon heating above its T_g [4]. The T_{cc} of all the blends was also observed in a temperature range of 104.4-115.5°C, which decreased continuously with increasing PBT loadings. This is probably due to the nucleating effect of PBT in the RPET and the increased free spaces in these immiscible blends that facilitated the mobility of the RPET segments to form

small crystallites, resulting in a decreased T_{cc} [4]. Additionally, the T_{cc} of all composites (Figure 6(a)) was found to be either higher or lower than that of the neat 60/40 (wt%/wt%) RPET/PBT blend and was in the temperature range of 103.3-107.4°C. This suggested that the WLN particles caused either enhanced crystallization (lower T_{cc}) due to the nucleation effect or delayed crystallization (higher T_{cc}) due to the restriction of RPET chain mobility, which limited the growth of polymer crystals. The T_m of the neat RPET and PBT derived from the first heating curves (Figure 5(a)) was found to be 248°C and 225°C, respectively, suggesting that the PBT had lower T_m than the RPET. This is again due to the shorter ethylene segment in RPET as discussed above. Thus, the neat RPET and PBT were semicrystalline polymers (exhibited both T_g and T_m), where their crystalline and amorphous phases could co-exist [23]. However, the T_m of RPET in all the blends and composites were found to be higher than that of the neat RPET, which may be due to the complete crystallization of RPET with the addition of both PBT and WLN. The T_m of the RPET in the blends and composites was found to be in a narrow range of 253.2-255.6°C and 251.4-253.7°C, respectively, suggesting that the addition of PBT and WLN had no significant effect on the melting behavior of RPET in the blends and composites. Moreover, the T_m of PBT in the blends at 10 and 20 wt% PBT was not visible due to the small amount of PBT in these blends, and so the T_m of PBT was not be detected, while at higher PBT loadings (30-50 wt%), the T_m of PBT could be found at a slightly lower temperature range (222.2-223.5°C) compared to that of the neat PBT. Meanwhile, the T_m of PBT in all the composites (221.5-223.6°C) was close to that of the neat 60/40 (wt%/wt%) RPET/PBT blend (223.5°C). The two distinct endothermic melting peaks of RPET and PBT that were observed in the blends at 30-50 wt% PBT and in all the composites suggested that RPET and PBT were not miscible in the crystalline region.

Table 2. DSC-derived data of the samples.

Sample	First heating				Cooling	Second heating
	T_g (°C)	T_{cc} (°C)	$T_{m,PBT}$ (°C)	$T_{m,RPET}$ (°C)	T_c (°C)	$T_{m,RPET}$ (°C)
RPET	74.5	120.0	-	248.0	210.0	233, 247
PBT	60.0		-	225.0	206.0	220.6
RPET/PBT (wt%/wt%)						
90/10	69.8	115.5	-	254.5	203.8	226.6, 239.3
80/20	68.0	110.8	-	253.5	199.7	218.0, 232.6
70/30	67.5	105.0	222.2	253.2	177.0	209.0
60/40	68.0	104.4	223.5	255.6	167.3	200.0
50/50	67.0	105.6	223.3	254.0	150.3	188.0
RPET/PBT/WLN (wt%/wt%/wt%)						
54/36/10	63.7	107.4	223.6	253.7	169.2	205.0
48/32/20	63.6	106.0	222.6	252.3	173.3	206.2
42/28/30	64.5	104.4	223.0	253.4	172.2	203.2
36/24/40	60.0	103.3	221.5	251.4	174.7	206.0
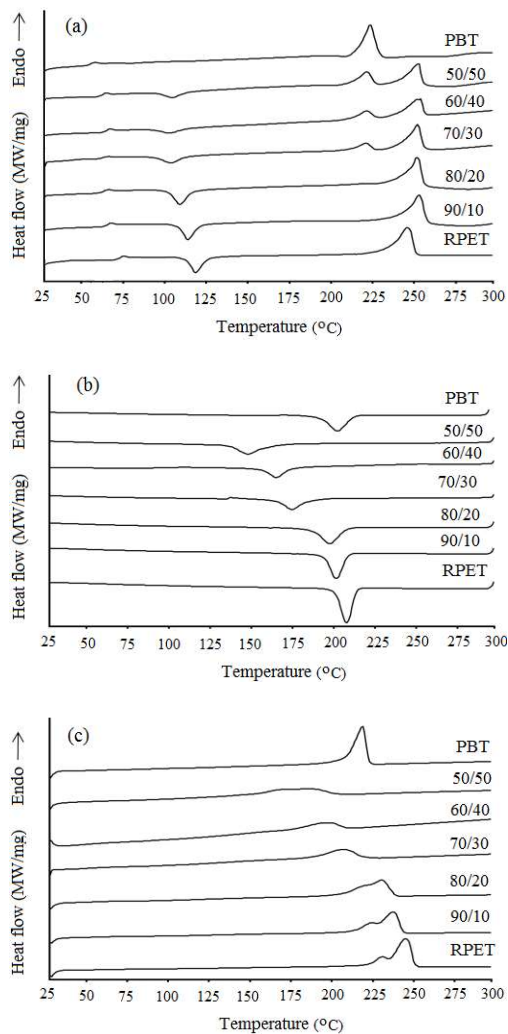
Figure 5. DSC thermograms of RPET, PBT and RPET/PBT blends obtained from (a) first heating scan, (b) cooling scan and (c) second heating scan.

From the cooling curves (Figure 5(b)), it is seen that the T_c of the neat RPET and PBT was 210 and 206°C, respectively, indicating that the RPET crystallized earlier than the PBT. This may be due to the reduction in the molecular weight of RPET by chain scission during heating that in turn facilitated its crystallization upon cooling [1]. It was also observed that all of the blends and composites exhibited a lower T_c than the neat RPET (Figures 5(b) and 6(b)), indicating that the crystallization of the RPET was delayed by the presence of PBT and WLN in a dose dependent manner. This suggested that the PBT and WLN particles obstructed the crystallization process of the RPET upon cooling.

From the second heating curves (Figure 5(c) and 6(c)), all the samples exhibited only the endothermic melting peaks. The double T_m peaks could be observed for the neat RPET and the blends at 10 and 20 wt% PBT [23]. Each sample exhibited a major T_m peak and a small shoulder at lower temperature. The T_m at lower temperature corresponded to the less perfect crystals of RPET that was able to melt in time and the recrystallized into the more perfect crystals and then re-melt at higher temperature [23].
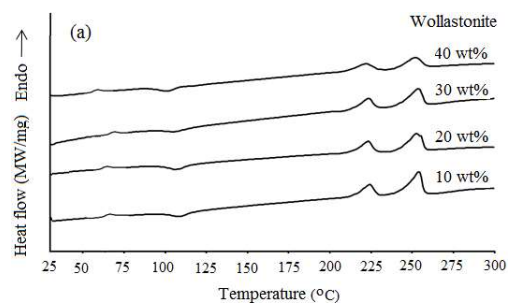
Figure 6. DSC thermograms of 60/40 RPET/PBT blend composites with WLN content of 10, 20, 30 and 40 wt% obtained from (a) first heating scan, (b) cooling scan and (c) second heating scan.
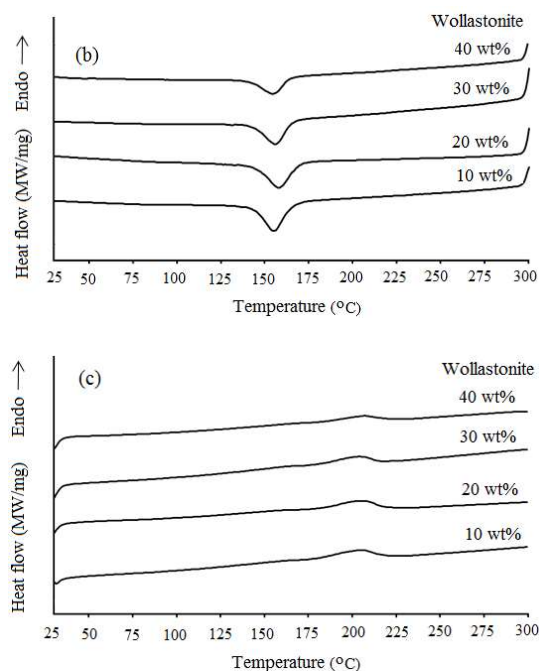
Figure 6. DSC thermograms of 60/40 RPET/PBT blend composites with WLN content of 10, 20, 30 and 40 wt% obtained from (a) first heating scan, (b) cooling scan and (c) second heating scan. (continued)

4. Conclusions.

Polymer blends and composites based on RPET, PBT and ultrafine WLN (~5 μm) were prepared on a co-rotating twin screw extruder and an injection molding machine with the aim of improving the toughness and stiffness of the RPET. The RPET use in this study was a pre-consumer waste (preform scrap) derived from the plastic bottle manufacturing industry. The incorporation of an appropriate amount of PBT in the RPET was found to simultaneously enhance both the impact strength and Young's modulus. The blend at 40 wt% PBT exhibited a good combination of mechanical properties in terms of stiffness and toughness due to a better PBT dispersion within the RPET matrix at this concentration that imparted high stress transfer and chain entanglement between RPET and PBT. As a consequence, the 60/40 (wt%/wt%) RPET/PBT blend was selected for preparing composites with four loading levels of the ultrafine WLN particles (10-40 wt%). It is seen that the incorporation of WLN, an inorganic filler with a high aspect ratio, remarkably increased the impact strength and Young's modulus of the resulting composites, especially at 30 wt% WLN, but a slight decrease in the tensile strength and elongation at break in a dose-dependent manner compared to the neat 60/40 (wt%/wt%) RPET/PBT blend. These results agree well with the morphology derived from the SEM analysis. DSC data reveals the miscibility in the amorphous region of the RPET and PBT and the immiscibility in the crystalline phases of the blends and composites.

References

[1] Y. Srithep, A. Javadi, S. Pilla, L. S. Turng, S. Gong, C. Clemons, and J. Peng, "Processing and characterization of recycled poly(ethylene terephthalate) blends with chain extenders, thermoplastic elastomer, and/or poly(butylene adipate-co-terephthalate)," *Polymer Engineering and Science*, vol. 51, pp. 1023-1032, 2011.

[2] I. Irska, S. Paszkiewicz, K. Gorący, A. Linares, T. A. Ezquerra, R. Jędrzejewski, Z. Rosłaniec, and E. Piesowicz, "Poly(butylene terephthalate)/ polylactic acid based copolyesters and blends: miscibility-structure-property relationship," *Express Polymer Letters*, vol. 14, pp. 26-47, 2020.

[3] M. Nofar and H. Oğuz, "Development of PBT/recycled-PET blends and the influence of using chain extender," *Journal of Polymers and the Environment*, vol. 27, pp. 1404-1417, 2019.

[4] S. Chuayjuljit, P. Chaiwutthinan, L. Raksaksri, and A. Boonmahitthisud, "Effects of poly(butylene adipate-co-terephthalate) and ultrafined wollastonite on the physical properties and crystallization of recycled poly(ethylene terephthalate)," *Journal of Vinyl and Additive Technology*, vol. 23, pp. 106-116, 2015.

[5] P. Chaiwutthinan , S. Suwannachot, and A. Larpkasemsuk, "Recycled poly(ethylene terephthalate)/polypropylene/wollastonite composites using PP-g-MA as compatibilizer: Mechanical, thermal and morphological properties," *Journal of Metals, Materials and Minerals*, vol. 28, pp.115-123, 2018.

[6] E. J. Velásquez, L. Garrido, A. Guarda, M. J. Galotto, and C. López de Dicastillo, "Increasing the incorporation of recycled PET on polymeric blends through the reinforcement with commercial nanoclays," *Applied Clay Science*, vol. 180, article 105185, 2019.

[7] S. Katoch, V. Sharma, and P. P. Kundo, "Synthesis and characterization of saturated polyester and nanocomposites derived fom glycolyzed PET waste," *Bulletin of Materials Science*, vol. 36, pp. 277-286, 2023.

[8] I. Acar, A. kaşgőz, S. Őzgűműs, and M. Orbay, "Modification of waste poly(ethylene terephthalate) (PET) by using poly(L-lactic

acid) (PLA) and hydrolytic stability," *Polymer-Plastics Technology and Engineering*, vol. 45, pp. 351-359, 2006.

[9]   P. Chaiwutthinan, S. Chuayjuljit, A. Boonmahitthisud, and A. Larpkasemsuk, "Recovery of recycled poly(ethylene terephthalate) via melt mixing with poly(butylene succinate) and ultrafine wollastonite," *Journal of Metals, Materials and Minerals*, vol. 29, pp. 69-77, 2019.

[10] K. Yamada and S. Thumsorn, "Effectiveness of talc filler on thermal resistance of recycled PET blend," *Advances in Materials Physics and Chemistry*, vol. 3, pp. 327-331, 2013.

[11] L. M. G. Guadagnini and A. R. Morales, "Compatibilization of recycled polypropylene and recycled poly(ethylene terephthalate) blends with SEBS-g-MA," *Polimeros*, vol. 28, pp. 84-91, 2018.

[12] P. Chaiwutthinan, A. Pimpong, A. Larpkasemsuk, S. Chuayjuljit, and A. Boonmahitthisud, "Wood plastic composites based on recycled poly(ethylene terephthalate) and poly(butylene adipate-co-terephthalate)," *Journal of Metals, Materials and Minerals*, vol.29, pp. 87-97, 2019.

[13] S. Mbarek and M. Jaziri, "Recycling poly(ethylene terephthalate) waste: properties of poly(ethylene terephthalate) /polycarbonate blends and the effect of a transesterification catalyst," *Polymer Engineering and Science*, vol. 46, pp. 1378-1386, 2006.

[14] W. Thodsaratpreeyakul, P. Uawongsuwan, and T. Negoro, "Properties of recycled-poly(ethylene terephthalate)/polycarbonate blend fabricated by vented barrel injection molding," *Materials Science and Applications*, vol. 9, pp. 174-190, 2018.

[15] Y. Lei, Q. Wu, and Q. Zhang, "Morphology and properties of microfibrillar composites based on recycled poly (ethylene terephthalate) and high density polyethylene," *Composites Part A: Applied Science and Manufacturing*,

[16] vol. 40, pp. 904-912, 2009.

[16] M. R. Raiisi-Nia, A. Aref-Azar, and M. Fasihi, "Acrylonitrile-butadiene rubber functionalization for the toughening modification of recycled poly(ethylene terephthalate)," *Journal of Applied Polymer Science*, vol. 131, pp. 40483, 2014.

[17] N. M. L. Mondadori, R. C. R. Nunes, L. B. Canto, and A. J. Zattera, "Composites of recycled PET reinforced with short glass fiber," *Thermoplastic Composite Materials*, vol. 25, pp. 747-764, 2011.

[18] P. R. Rajakumar and R. Nanthini, "Thermal and morphological behaviours of polybutylene terephthalate/polyethylene terephthalate blend nanocomposites," *RASĀYAN Journal of Chemistry*, vol. 4, 567-579, 2011.

[19] R. N. Baxi, S. U. Pathak, and D. R. Peshwe, "Impact modification of a PET-PBT blend using different impact modifiers," *Polymer Journal*, vol. 43, pp. 801-808, 2011.

[20] G. S. Deshmukh, D. R. Peshwe, S. U. Pathak, and J. D. Ekhe, "Evaluation of mechanical properties and thermal properties of poly(butylene terephthalate) (PBT) composites reinforced with wollastonite," *Transactions of the Indian Institute of Metals*, vol. 64, pp. 127-132, 2011.

[21] A. Wozniak-Braszak, K. Jurga, J. Jurga, M. Baranowski, W. Grzesiak, B. Brycki, and K. Hołderna-Natkaniec, "Effect of fullerene derivates on thermal and crystallization behavior of PBT/decylamine-C_{60} and PBT/TCNEO-C_{60} Nanocomposites," *Journal of Nanomaterials*, vol. 2012, Article ID 932573.

[22] K. P. Chaudhari and D. D. Kale, "Impact modification of waste PET by polyolefinic elastomer," *Polymer International*, vol. 52, pp. 291-298, 2003.

[23] A. R. McLauchlin and O. R. Ghita, "Studies on the thermal and mechanical behavior of PLA-PET blends," *Journal of Applied Polymer Science*, vol. 133, pp. 44147, 2016.